World Journal of Engineering and Technology, 2023, 11, 303-318
https://www.scirp.org/journal/wjet
ISSN Online: 2331-4249
ISSN Print: 2331-4222

Comparisons of Structured Surface Floors for Pool Boiling Enhancement at Low Heat Fluxes: Hands-On Learning Setup for Heat Transfer Classroom

Birce Dikici[1]*, Basim Q. A. Al-Sukaini[2]

[1]Department of Mechanical Engineering, Embry-Riddle Aeronautical University (ERAU), Daytona Beach, FL, USA
[2]Rumaila Operating Organization (ROO) HQ, Basra Oil Company (BOC) Rumaila, Basra, Iraq
Email: *dikicib@erau.edu

How to cite this paper: Dikici, B. and Al-Sukaini, B.Q.A. (2023) Comparisons of Structured Surface Floors for Pool Boiling Enhancement at Low Heat Fluxes: Hands-On Learning Setup for Heat Transfer Classroom. *World Journal of Engineering and Technology*, **11**, 303-318.
https://doi.org/10.4236/wjet.2023.112022

Received: March 16, 2023
Accepted: May 14, 2023
Published: May 17, 2023

Abstract

Various enhanced surfaces have been proposed over the years to improve boiling heat transfer. This paper introduces an experimental setup designed for boiling demonstration in the graduate-level Heat Transfer course. The pool boiling performance of water under atmospheric pressure of 1.025 bar is investigated by using several structured surfaces at heat fluxes of 28 and 35 kW/m^2. Surfaces with holes, rectangular grooves, and mushroom fins are manufactured by an NC-controlled vertical milling machine. The heat flux versus excess temperature graph is plotted by using thermocouple measurements of water and base temperatures of the boiling vessel. The separation, rise, and growth of individual vapor bubbles from the surface during boiling were recorded with a digital camera. The results for the plain surface are compared to the Rohsenow correlation. The enhancement of heat transfer coefficient (h) ranged between 15% - 44.5% for all structured surfaces. The highest heat transfer coefficient enhancement is observed between 41% - 56.5% for holed surface-3 (405 holes) compared to the plain surface. The excess temperature dropped around 29% - 34% for holed surface-3 (405 holes) compared to the plain surface. The heat transfer coefficient increases as the spacing between channels or holes decreases. While the bubbles on holed and mushroomed surfaces were spherical, the bubbles on the flat and grooved surfaces were observed as formless. The suggested economical test design could be appropriate to keep students focused and participating in the classroom.

Keywords

Boiling, Pool Boiling, Heat Transfer Coefficient, Enhancement Techniques,

Engineering Education

1. Introduction

Nucleate boiling is defined by the liquid-vapor phase change and the associated bubble formation. Since boiling is an effective heat transfer mode, it has many uses in engineering fields. Small temperature gradients can transfer high heat flux in evaporators. The high heat generation in electronic parts should be prevented because high heat causes performance decrease and malfunction of the parts. Compared to other types of heat transfer that do not involve phase change, a much larger amount of heat can be removed with a low-temperature change during boiling [1].

Techniques for improving the boiling are divided into passive and active. Passive techniques improve the boiling heat transfer with surface modifications. This can be through macro, micro, and nanochannels, fins, porous layer coating, such as metallic foams, hydrophobic and hydrophilic surfaces, and re-entrant cavities. The re-entrant cavities capture the vapor continuously and contribute to the nucleation process, thereby increasing the heat transfer performance [2]. Examples of active techniques are surface and fluid vibration, surface rotation, and the use of an electric field [3]. However, these methods were not developed because they found few practical applications. It is also possible to increase boiling heat transfer by adding surfactants. Several studies improved the pool boiling heat transfer of water by adding surfactant Sodium Lauryl Sulfate (SLS) and environmentally friendly surfactants such as ECOSURF™ EH-14 and SA-9 [4] [5] [6].

Some researchers conducted a study to investigate the performance of enhanced surfaces in nucleate pool boiling. The experimental results showed that the surfaces with inclination performed better compared to the ones normal to the surface [7]. Pool boiling experiments were conducted at three heating surfaces with seven different incline angles by Wang *et al.* [8]. CHF is reduced for the incline angle of the heating surface for $\theta > 90^\circ$. The bubble diameter increases with the increase of inclination angle accompanied by a lower frequency and lower sliding time [8]. Using the HFE 7100 engineering fluid, Filho *et al.* [9] investigated the thermal performance of surfaces with micron and nanometer fins. The boiling tests on micro-nano hybrid surfaces (*i.e.*, hierarchically structured surfaces) indicated a significant enhancement in the heat transfer coefficient due to improved nucleation site density and vapor bubble dynamics [9]. Sia *et al.* [10] applied nanocomposite coatings to enhance the subcooled flow boiling heat transfer in a mini channel. The nanocomposites had tunable wettability, such as super hydrophilic, superhydrophobic, and hydrophobic [10]. The super hydrophilic graphene nanoplatelets (GNPs) coating showed a boiling heat transfer coefficient with an enhancement of 64.9% [10]. However, the hydrophobic and superhydrophobic GNPs coatings deteriorated the flow boiling rates [10].

Shahmardi *et al.* [11] studied the role of surface topology and surface chemistry on the onset of boiling with a novel setup. They considered a hydrophilic and hydrophobic wall and two wall topologies, a flat wall and a wall with a periodic array of nanocavities [11]. The presence of nanostructures triggered the bubble formation for a hydrophilic wall and postponed it for a hydrophobic wall [11]. A hydrophilic surface provided better energy transfer from the hot wall to the water [11]. Moze *et al.* [12] created surface models consisting of low and high-wettable areas to improve boiling. These special surfaces increased the critical heat flux and heat transfer coefficient. The created surfaces were found suitable for high heat flux applications [12].

Zupancic *et al.* [13] partitioned the heat flow during boiling on thin metal substrates. They created nucleation sites using the nanosecond fiber laser texturing method. However, their investigations did not show noticeable differences in bubble radius, bubble growth, and nucleation temperature on these surfaces [13].

Jayaramu *et al.* [14] [15] investigated the oxidation of copper channels in a boiling stream and designed a dual-phase microchannel heat sink from copper. They recorded the change in surface characteristics by using a profilometer, confocal microscope, SEM, EDX, and XRD. They found that the growth of an oxide layer on the walls increases the wettability of the surface and therefore negatively affects the boiling.

Complex geometries for the boiling wall can be produced by additive manufacturing (3D printing) [10]. While this may seem like a very promising innovation, there are many difficulties in creating and controlling complex geometries [10].

Sielaff *et al.* [16] performed multi-scale boiling experiments using fully fluorinated liquid FC-72 on the International Space Station. The growth of bubbles during boiling, the effect of shear flow, and the effect of the electric field were investigated [17]. Their studies have shown that the bubble rupture volume depends on the intensity of the electric field, while the bubble rupture depends on the pressure, subcooling, and heat flow [17].

In the current work, nucleate pool boiling on several macro-structured surface floors with distilled water under atmospheric pressure is evaluated. Other researchers focused mostly on boiling on micro and nanostructured surfaces. As a novelty, the experimental setup is introduced for engineering education. The aims of this investigation are summarized below:

1) Conduct experiments to compare boiling performances of plain and enhanced surface floors (*i.e.* floors with rectangular channels, holes, and mushroom fins of various sizes.)

2) Discuss the boiling phenomena using observations and referring to the theory.

3) Introduce the experimental test setup to be used in classrooms to improve engineering education through a hands-on laboratory learning approach.

Engineering education aspect:

Previous research has proven that students learn better with hands-on approaches than with traditional methods [18]. Instructors strive to teach hands-on because they expect their students to be future innovators of society [19]. Hands-on activities can be used in engineering classes to increase student participation and to better understand the subject and concepts. This method of learning is suitable for engineering students as it can be similar to the devices they will use in their future careers. Including such activities in the classroom is usually hindered by financial difficulties, sophisticated, large, and heavy devices, and lack of time [19] [20].

Pour *et al.* [20] and Dahlke *et al.* [19] have developed low-cost desktop learning modules for Fluid Mechanics and Heat Transfer courses (Miniaturized industrial equipment such as fluidized bed, Venturi System, Cross Flow Heat Exchanger, Tubular Heat Exchanger, Shell and Tube Heat Exchanger units, and hydraulic system energy loss unit). Adesope *et al.* [18] evaluated students' cognitive effort when low-cost desktop learning modules (LC-DLMs) are used. Students discussed with each other, asked, and answered questions, and brought clarity to the learning. Toro *et al.* [21] developed a solar-powered direct steam generation boiler for an educational desktop Rankine Cycle. They developed a thermal model to characterize the concentrated solar power and heat transfer to the working fluid. They analyzed and validated the solar-to-steam efficiency with a small size economical device.

The suggested test setup will help students understand key concepts about boiling heat transfer. Target students will be from graduate-level Heat Transfer classrooms. The classroom sections consist of 50 minutes, thrice-weekly instruction in Heat Transfer (If undergraduate level Heat Transfer course is given as two courses of Heat Transfer I and Heat Transfer II, then the activity could be included in Heat Transfer II).

2. Materials and Methods

2.1. Boiling Vessel and Structured Surfaces (*i.e.*, Floors)

The experimental set-up, shown in **Figure 1**, consists of a hot plate, a boiling vessel, a ruler, thermocouples, and a digital camera. The boiling vessel has dimensions of 5.25 inches (13.34 cm) in length, 4.5 inches (11.43 cm) in height, 3.5 inches (8.89 cm) in width, and 0.25 inches (0.64 cm) in thickness. The boiling vessel has two pieces of borosilicate transparent glass. Borosilicate glass is a suitable material for a boiling vessel because it is transparent, has a low thermal expansion, and can resist high temperatures (450˚C) for a long time. Two pieces of borosilicate glass are inserted in the slots at the edges of the surface floor. The remaining surfaces are made of aluminum, and they were attached with screws and sealed with silicone to prevent leakage.

NC-controlled vertical milling machine is used to make the structured surfaces floors in the machine shop. For holed surfaces, a drill chuck is used to drill the holes. The grooves on the surfaces were made with a right-angle head attachment using a slitting saw. For obtaining the mushroomed surface, round-head rivets were pressed into the drilled holes in the surface.

The surface floors are varied by changing the fin length and fin spacing. The structured surface floors are shown in **Figure 2** and **Figure 3**. The boiling vessel has the specified structured surface plate manufactured separately by reassembling the bottom surface (*i.e.* floor) as a structured surface. **Figure 3** and **Table 1** show the properties of the structured surfaces. To understand the effect of spacing, the dimensionless parameter (β) is used to compare boiling performance from the surfaces in **Figure 2** and **Table 1**, similar to Das *et al.* [7]. As the spacing decreases, β decreases as well. The area augmentation ratio, A_r is given in Equation (1). The spacing (S) to depth (D) ratio, β, is calculated for all surfaces by Equation (2):

$$A_r = \frac{A_{augmented}}{A_{plain}} \tag{1}$$

$$\beta = S/D \tag{2}$$

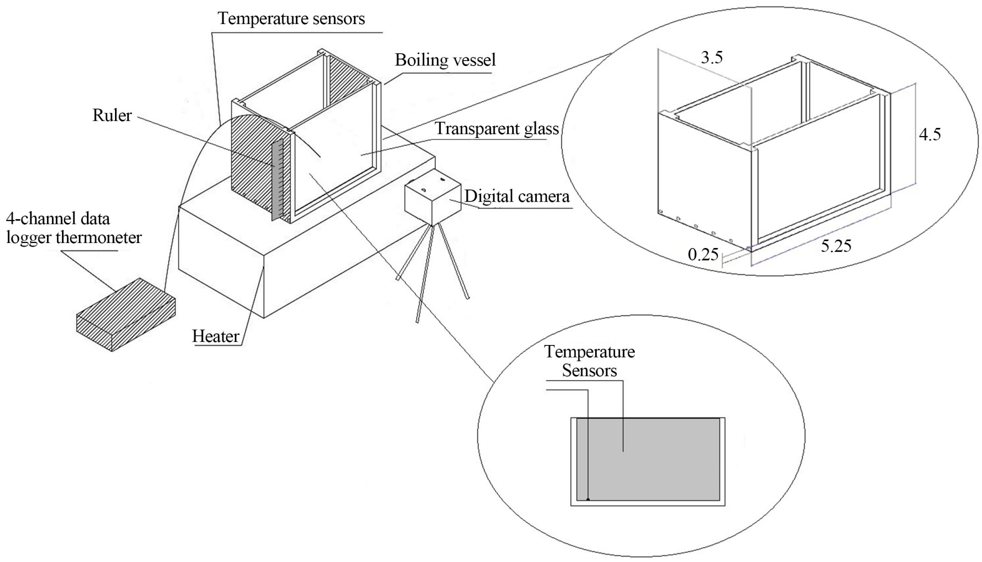

Figure 1. Experimental test setup (dimensions are in inches).

Table 1. Properties of structured surface floors.

Surfaces	# of channels/holes/ mushroom fins	Area augmentation ratio (A_r)	β
Plain	---	1	--
Mushroomed	45 mushroom fins	1.12	1.67
Holed 1	77 holes	1.15	2
Holed 2	187 holes	1.37	1
Holed 3	405 holes	1.81	0.5
Grooved 1	9 channels	1.328	3.75
Grooved 2	17 channels	1.62	2
Grooved 3	27 channels	1.98	1

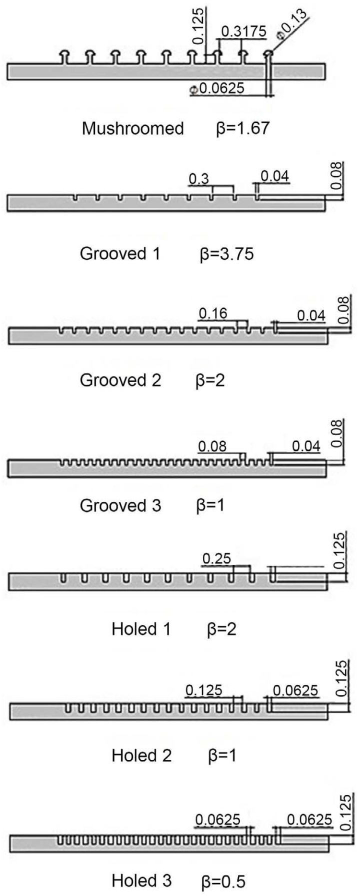

Figure 2. Cross-sectional dimensions of structured surfaces (in inches).

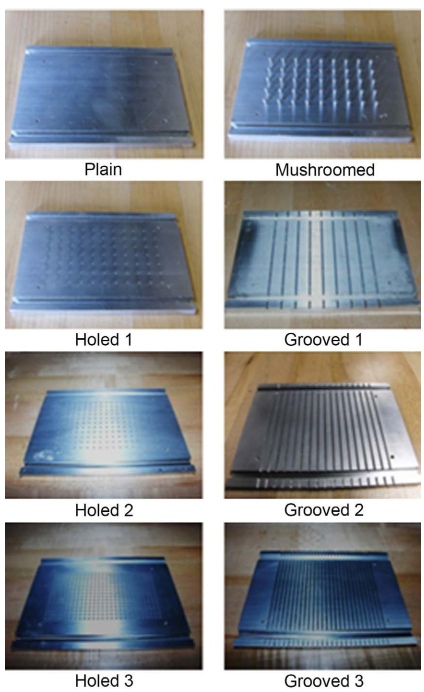

Figure 3. Structured surface floors (Image: [22]).

2.2. Test Procedure

A type-K thermocouple was mounted to the base of the boiling vessel to measure the vessel's interior bottom surface (*i.e.* floor). This thermocouple has a self-adhesive foil backing for a faster response time. The boiling vessel was filled with a measured quantity of distilled water (400 gr). The other type-K thermocouple is clipped from the edge of the vessel to measure the water temperature (**Figure 1**). The boiling vessel is placed on Benchmark hot plate. The base material and the surface of the hot plate are cast aluminum and ceramic coating, respectively.

The heat flux was adjusted from the hot plate and the water was left to boil. The PC acquires and displays the temperature sensor readings. The RDXL4SD model temperature logger collects temperature information and converts it to an Excel file. The boiling vessel enables clear viewing and allows observation of the amount of liquid evaporated. The atmospheric pressure is measured as 1.025 bar.

Casio EX-FH20 digital camera was placed in front of the boiling vessel and the bubble dynamics of the boiling were examined. The camera is capable of capturing 1000 frames per second of video and can continuously take high-resolution pictures, (40 images per second). Flush continuous shutter mode helped to record consecutive images while firing the flash. After continuous shutter shooting is finished, the images are examined for evaluating the bubbles.

2.3. Governing Equations

The defining characteristics of boiling are the temperature change at the surface, the boiling curve, the boiling mode, and the critical heat flux. If the temperature of the liquid is less than the saturation temperature, T_{sat} boiling is called "subcooled boiling" and the heat is transferred as sensible heat. The heat transfer from the hot surface to the water brings the temperature of the water, T_i to the saturation temperature, T_{sat} [23]; ΔT is the temperature difference. In Equation (3) $q''_{subcooled}$ is the net heat transfer from the hot plate to the water.

$$q''_{subcooled} = \frac{mc_p \Delta T}{A \Delta t} \tag{3}$$

When the temperature of the liquid reaches the saturated temperature, the boiling is called "saturated boiling". At saturated boiling, the heat transfer to liquid is used for phase change [23]. Equation (4) relates the heat from the base plate, $q''_{subcooled}$, to the convective heat transfer to the water. It equates the same heat, q''_{sat} to the heat escaping during boiling mass transfer in Equation (4).

$$q''_{sat} = h\left(T_S - T_{sat}\right) = h\Delta T_e = \frac{\dot{m}_b h_{fg}}{A} \tag{4}$$

Equation (5) is developed by Rohsenow and is the first correlation for nucleate boiling [23]. The coefficient $C_{s,f}$ and the exponent n are coefficients depending on the solid-liquid combination.

$$q_s'' = \mu_l h_{fg} \left[\frac{g(\rho_l - \rho_v)}{\sigma} \right]^{1/2} \left(\frac{c_{p,l} \Delta T_e}{C_{s,f} h_{fg} \Pr_l^n} \right)^3 \tag{5}$$

In Equation (5), the proportionality of $\Delta T_e \propto (q_s'')^{1/3}$ shows the increasing ability of the interface to transfer heat. If there is a one-dimensional heat transfer from the hot surface to the water at a steady flow, the flow is given by Fourier's law [23]:

$$q_s'' = -k \frac{\partial T}{\partial x} = -k \frac{\Delta T}{\Delta x} \tag{6}$$

With the temperature difference between the boiling vessel bottom and the boiling vessel inlet measured, the heat flux is calculated, and it is the heat flux is delivered to the liquid. The heat transfer coefficient, *h,* is calculated from Equation (4).

The power depends on current, which is the rate of charge flow past a given area called an electric current, and potential difference. The power (determined as $P = I \times V$) is the heat transfer rate from the heater.

There are four boiling regimes in the pool watering curve, depending on excess temperature, ΔT, and the difference between the surface temperature, T_s, and the saturation temperature, T_{sat} [17]. When the excess temperature, ΔT, reaches between 1˚C - 5˚C, heat is transferred from the solid surface to the bulk liquid via natural convection currents [24]. The liquid becomes slightly superheated, rises to the surface, and evaporates afterward [17]. When the excess temperature, ΔT, reaches between 5˚C - 30˚C, the boiling is called nucleate boiling [25]. If the excess temperature, ΔT, stays between 5˚C - 10˚C, it is called an "isolated bubble" regime, and convection remains the primary mechanism. Each bubble generated can grow and detach from the surface without interaction with other bubbles. As the excess temperature, ΔT increases over 12˚C, extra nucleation sites become active, generating more bubbles. Bubbles merge and form columns and slugs of vapor [24].

Once the spherical bubble is considered, the vapor is at a pressure p_v inside the bubble. Outside of the bubble, the liquid pressure is p. The pressure force must be balanced by the surface tension force, which is the product of the circle's circumference, $2\pi R$, and the surface tension, σ [17]. This is given in Equation (7).

$$(p_v - p) = \frac{2\sigma}{R} = \frac{4\sigma}{D} \tag{7}$$

When the bubble within the liquid is heated, the pressure of this vapor is equal to p_v. If the pressure of this liquid is p, then the liquid temperature is less than the vapor temperature. Therefore, heat is transferred from the vapor to the surrounding liquid. Thus, the vapor condenses, and the bubble bursts. However, if the liquid temperature is higher than the vapor temperature, the bubble rises upwards from the hot surface (Region II) [17].

2.4. Uncertainty

It was aimed to minimize the uncertainty in the experimental measurements. Accuracy is generally associated with repeatable and fixed errors while precision is associated with unrepeatable and random errors. Following the uncertainty methodology, there are two types of error: (1) Systematic (*i.e.*, bias) error occurs when there is a fault in the device or the system that processes the values. A systematic error occurs when the experimenter uses the instrument incorrectly, as well. (2) Random (*i.e.*, precision) errors in experiments are caused by unknown and unpredictable differences in the experiment. These errors may be caused by the device or by environmental conditions. An example of random error is the electric noise in the circuit of the electrical device [26]. For example, poor heat contact between the sensor and the object being measured causes values to be read incorrectly. In this study, the measured quantities are surface and water temperatures measured by thermocouples. The K-type thermocouples lead to uncertainties in the results. The calculated quantity is heat flux, q'', and the enthalpy, h.

The tolerance value for the type-K thermocouple is ±(0.4% +1˚C). The response time of the K-type thermocouples is 0.002 seconds in still water. The Type-K thermocouple was calibrated in water from ambient temperature, 20˚C to the boiling temperature of the water, 100˚C, by comparing it with another thermocouple. The differences between the K-type thermocouple and calibrated thermocouples are between 0.1˚C - 2.1˚C. Material with high thermal conductivity was used between the thermocouple and the hot plate to prevent random error.

RDXL4SD 4-channel datalogger thermometer has an accuracy of ±(0.4% + 1˚C) and Benchmark hot plate has a precise temperature control of ±1˚C, as reported by the manufacturer.

Boiling heat transfer experiments can involve significant uncertainty. The measured surfaces are assumed to have the same roughness on the surface. Each experiment was repeated at least three times to ensure consistency and accuracy in the experiments. For the scope of this paper, two points for the boiling curve are obtained for two heat fluxes. It would be more accurate to add more points at different heat fluxes.

The experimental data for plain surfaces are compared to the predictions made by the Rohsenow correlation in Equation (5) [23]. With the viscosity of water, $\mu_l = 279 \times 10^{-6}$ (N·s/m^2), latent heat of vaporization, $h_{fg} = 2257 \times 10^3$ (J/kg), gravitational acceleration, $g = 9.81$ (m/s^2), liquid density, $\rho_l = 957.9$ (kg/m^3), vapor density, $\rho_v = 0.5956$ (kg/m^3), surface tension, $\sigma = 58.9 \times 10^{-3}$ (N/m), specific heat at constant pressure $c_{p,l} = 4.217 \times 10^3$ (J/kg·K), the surface-fluid combination coefficient, $C_{s,f} = 0.011$, the exponent, $n = 1.26$ water-Aluminum (plate, oxidized) [27], and Prandtl number, $\Pr_l = 1.76$, this equation gives $q_s'' = 145.424(\Delta T_e)^3$ (W/m^2).

3. Results

Heat flux to excess temperature graph of structured surfaces is shown in **Figure 4**.

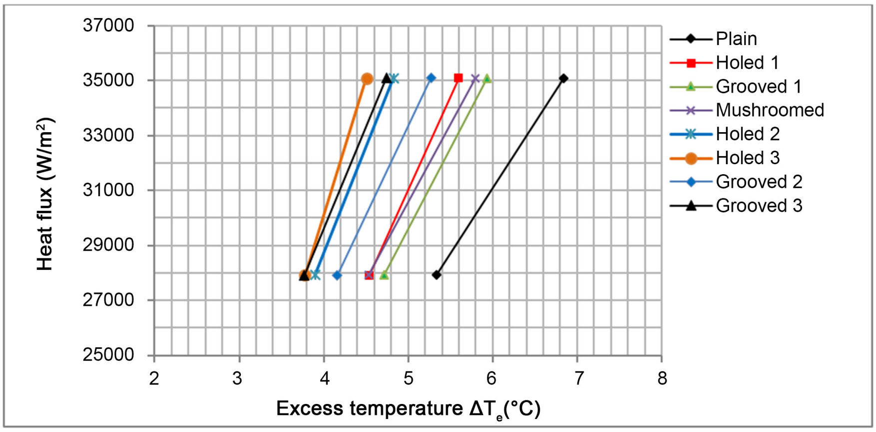

Figure 4. Pool boiling data of structured surfaces.

The spacing between the channels and holes is observed to affect the heat transfer. The images showing the bubble formation before reaching the boiling point are given in **Figure 5**. Examples of bubble diameter measurements at a heat flux of 35.08 kW/m^2 are presented in **Figure 6**. **Figure 7** shows the boiling on plain and structured surface floors at two values of heat flux.

4. Discussion

Figure 4 shows that heat flux versus excess temperature plots are shifted to the left for all structured surfaces. The heat transfer coefficient increased as the number of holes and grooves increased for holed and grooved surfaces. For a heat flux of 35.08 kW/m^2, *Holed* 3 surface shows the maximum heat transfer enhancement. It is about a 51.75 % increase in the heat transfer coefficient compared to the plain surface, while it was a 44.3% increase for the *Grooved* 3 surface. The enhancements in heat transfer coefficient for *Grooved* 1 and *Mushroomed* surface are 13.1% and 17.8%, respectively.

The nucleation sites are usually small gaps and cracks on the hot surface that can only be seen with a microscope. Nucleation generally occurs continuously in these places. As shown in Equation (7), the bubble diameter reaching a certain size is a function of the surface tension and pressure of the liquid at the liquid-vapor interface. Depending on the difference between the temperature of the hot plate and the saturation temperature, the bubbles either burst or rise by leaving the wall surface. **Figure 5** and **Figure 7** show that *Holed* 1 (77 holes) has more regularly distributed nucleation bubbles compared to other surfaces. The nucleation site densities for structured surfaces are higher compared to the smooth surface. This result is consistent with Das *et al.* [28]. *Holed* 3 surface showed higher nucleation site density compared to other surfaces. The bubbles that formed were smaller than the ones on the plain surface and they left the surface faster. This bubble size and high ascent rate were also observed at high heat flow and higher surface temperature.

For the plain surface, The Rohsenow correlation and our results in **Figure 4** do not agree extremely well. The error of Rohsenow correlation is 20.66 % at low heat flux and 32.66% at high heat flux for plain surface for n = 1.26. Liquid/surface combinations and surface roughness affect the coefficient $C_{s,f}$, and n significantly [27] [29]. For example, Piero *et al.* [27] reported that n = 1 for water/aluminum for polished circular plates and n = 1.26 for oxidized plates [27].

The amount of air in the water also influences the excess temperature. The more air there is in the vessel, the less water is in contact with the hot plate. In this case, more bubbles would be observed. The cavity is a stable vapor trap and has a positive effect on nucleation. This is explained as a reduction in the incipient boiling superheat and the increase of heat transfer in the nucleated boiling zone [7]. Surface finish, surface wettability, surface impurity, gravity, and thermal properties affect the heat transfer coefficient [30]. The roughness of the surface pulls the boiling curves to the left. However, wettability prevents nucleation and pulls the boiling curves to the right [30].

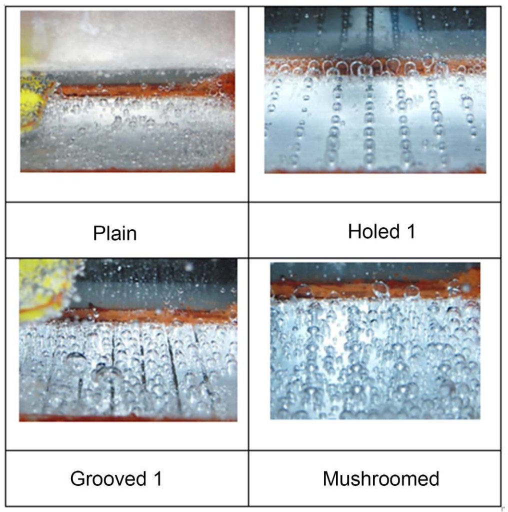

Figure 5. Images before reaching the boiling point (Image: [22]).

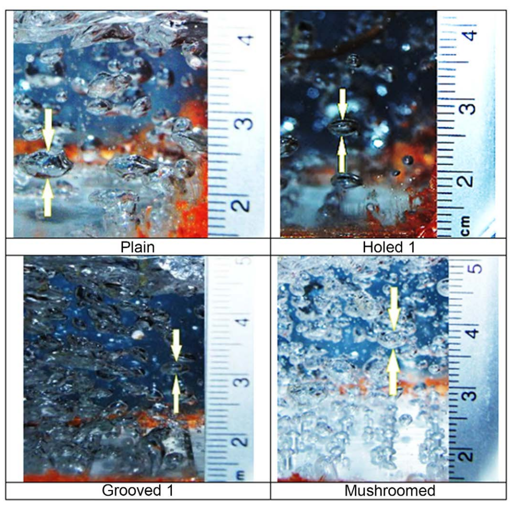

Figure 6. Measurement of bubble rise diameters at a heat flux of 35.08 kW/m^2 (Image: [4]).

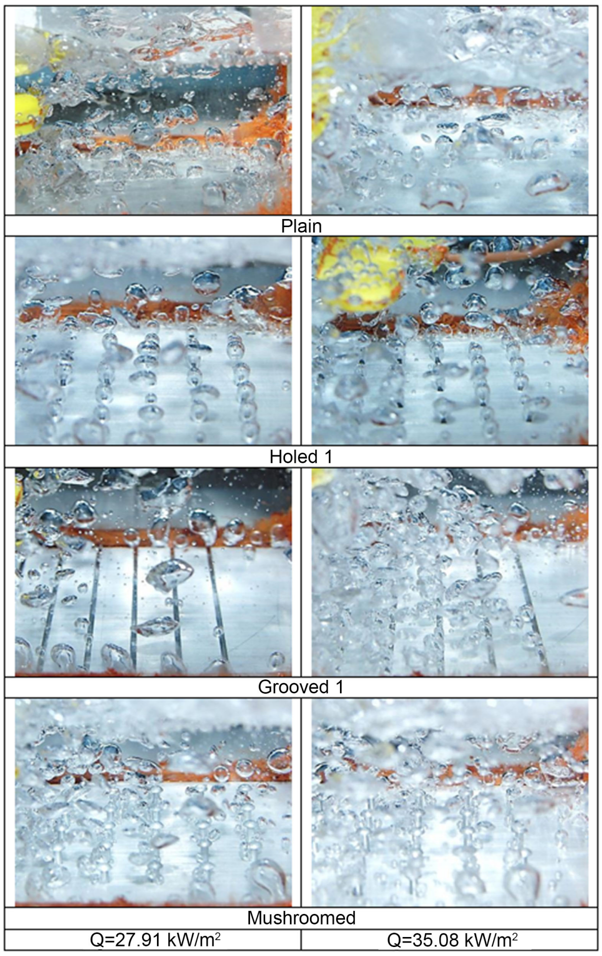

Figure 7. Boiling phenomena at different heat flux values (Image: [4]).

The experimental test setup described in this study could serve as an economical tool for demonstrating boiling heat transfer to students. The design enables performing an experimental process and increases students' scientific perception. Students observe and qualify different modes of boiling heat transfer. The dynamics of vapor bubble formation affect liquid motion near the floor surface and therefore influence the heat transfer coefficient. Another way to evaluate the boiling process is by the formation of growing and detaching bubbles from the surface. Vapor bubble growth and dynamics depend on various factors such as the excess temperature, the nature of the surface, and the thermophysical properties of the fluid.

This setup will help to prove the validity of the boiling equation and correlations in the textbook and to determine the experimental uncertainty for the plain surfaces. For structured surfaces, the following exercises are suggested for the classroom:

• Measure how the interior bottom (*i.e.* floor) temperature changes for the plain floor and when structured surfaces are replaced the plain floor at the given heat fluxes.

• For each surface, two data points appear in **Figure 4**. Plot a boiling curve by adding a few more data points using different heat fluxes.

• Describe how the bubbles form at structured surfaces compared to the bubbles at the plain surface. Students could take pictures and record videos using their smartphones. After the experiment is over, the shape and size of the bubbles could be compared and evaluated.

• Determine the effect of hole frequency or groove frequency on the change of base temperature and bubble formation.

5. Conclusions

The effect of structured geometries on pool boiling is investigated experimentally. Shifting the boiling curves to the left is favorable for heat flow because this shows that the heat transfer is increased. This also means that a large amount of heat transfer occurs at low surface temperatures.

The increase in heat transfer coefficient depends on the increase in the surface area and the shape of the protrusion. The lower the spacing-to-height ratio of the surfaces, the higher the measured heat transfer coefficients. The heat transfer enhancement at low heat fluxes can be because of increased nucleation site density and more efficient bubble departure dynamics. The plain surface does not have structures, so there are no additional nucleation sites to activate.

The following conclusions were drawn after analyzing the experimental results:

• The maximum enhancement in heat transfer coefficient ranged between 41% - 51.6% is measured by the *Holed*-3 surface (405 holes) and *Grooved*-3 surface compared to the plain surface (at 28 and 35 kW/m^2 heat fluxes).

• The excess temperature dropped for different surfaces compared to the plain surfaces. The highest excess temperature drop is around 29% - 34% for the *Holed*-3 surface (405 holes) compared to the plain surface at 28 and 35 kW/m^2 heat fluxes.

• The heat transfer coefficient increases as the spacing between channels or holes decreases.

• On surfaces with round and mushroom-shaped protrusions, the bubbles are usually spherical. It was observed that the bubbles on the flat and grooved surfaces were formless.

This study dealt with the physical conditions related to boiling and provided a foundation for performing relevant heat transfer calculations. A design and hardware validation of a boiling vessel that enables macro-structured surface floor modification is described. The design can improve engineering education through a hands-on learning approach in the classrooms. In the future, the effectiveness of the boiling test setup for learning could be explored.

Author Contributions

Conceptualization, B.D.; methodology, B.D. and B.Q.A.S.; formal analysis, B.D. and B.Q.A.S.; investigation, B.D. and B.Q.A.S.; resources, B.D.; data curation, B.D. and B.Q.A.S.; writing—original draft preparation, B.Q.A.S; writing—review and editing, B.D.; visualization, B.Q.A.S.; supervision, B.D.; funding acquisition, B.D. All authors have read and agreed to the published version of the manuscript.

Funding

Grant and support provided by Embry-Riddle Aeronautical University-Internal award (ERAU 13295) are gratefully acknowledged.

Acknowledgements

All the work was conducted in the Energy Systems Laboratory at ERAU. We thank the machinist, Mr. William Russo for manufacturing the parts of the boiling vessel and structured surface floors. The grant and support provided by ERAU are gratefully acknowledged.

Conflicts of Interest

The authors declare no conflicts of interest regarding the publication of this paper.

References

[1] Phan, H.T., Caney, N., Marty, P., Colasson, S. and Gavillet, J. (2009) How Does Surface Wettability Influence Nucleate Boiling? *Comptes Rendus Mecanique*, **337**, 251-259. https://doi.org/10.1016/j.crme.2009.06.032

[2] Mehta, J.S. and Kandlikar, S.G. (2012) Heat Transfer Enhancement during Pool Boiling of Water over Horizontal and Vertical Tubes with Micro Structured Surfaces. *Proceedings of the ASME* 10*th International Conference on Nanochannels*, *Microchannels*, *and Minichannels*, Rio Grande, 8-12 July 2012, 71-80. https://doi.org/10.1115/ICNMM2012-73175

[3] Mahmoud, M.M. and Karayiannis, T.G. (2021) Pool Boiling Review: Part I—Fundamentals of Boiling and Relation to Surface Design. *Thermal Science and Engineering Progress*, **25**, Article ID: 101024. https://doi.org/10.1016/j.tsep.2021.101024

[4] Al-Sukaini, B. (2014) Enhancement Techniques for Boiling Heat Transfer. Master's Thesis, ERAU, Daytona Beach.

[5] Dikici, B., Eno, E. and Compere, M. (2014) Pool Boiling Enhancement with Environmentally Friendly Surfactant Additives. *Journal of Thermal Analytic Calorimetry*, **116**, 1387-1394. https://doi.org/10.1007/s10973-013-3634-x

[6] Dikici, B. and Al-Sukaini, B.Q.A. (2018) Evaluations of Surfactant Solution for Nucleate Pool Boiling at Low Heat Fluxes. *Current Analysis on Chemistry*, **1**, 20-26.

[7] Das, A.K., Das, P.K. and Saha, P. (2009) Performance of Different Structured Surfaces in Nucleate Pool Boiling. *Applied Thermal Engineering*, **29**, 3643-3653. https://doi.org/10.1016/j.applthermaleng.2009.06.020

[8] Wang, C., Li, P., Zhang, D., Tian, W., Qiu, S., Su, G.H. and Deng, J. (2022) Experimental Study on the Influence of Heating Surface Inclination Angle on Heat Transfer and CHF Performance for Pool Boiling. *Nuclear Engineering and Technology*, **54**, 61-71. https://doi.org/10.1016/j.net.2021.07.033

[9] Filho, E.S., Kiyomura, I.S. andrade, B.A. and Cardoso, E.M. (2021) Pool Boiling

Performance of HFE-7100 on Hierarchically Structured Surfaces. *Case Studies in Thermal Engineering*, **2**, Article ID: 101536. https://doi.org/10.1016/j.csite.2021.101536

[10] Sia, G.D., Tan, M.K., Chen, G.M. and Hung, Y.M. (2021) Performance Enhancement of Subcooled Flow Boiling on Graphene Nanostructured Surfaces with Tunable Wettability. *Case Studies in Thermal Engineering*, **27**, Article ID: 101283. https://doi.org/10.1016/j.csite.2021.101283

[11] Shahmardi, A., Tammisola, O., Chinappi, M. and Brandt, L. (2021) Effects of Surface Nanostructure and Wettability on Pool Boiling: A Molecular Dynamic Study. *International Journal of Thermal Sciences*, **167**, Article ID: 106980. https://doi.org/10.1016/j.ijthermalsci.2021.106980

[12] Moze, M., Zupancic, M. and Golobic, I. (2020) Pattern Geometry Optimization on Superbiphilic Aluminum Surfaces for Enhanced Pool Boiling Heat Transfer. *International Journal of Heat and Mass Transfer*, **161**, Article ID: 120265. https://doi.org/10.1016/j.ijheatmasstransfer.2020.120265

[13] Zupancic, M., Gregorcic, P., Bucci, M., Wang, C., Aguiar, G.M. and Bucci, M. (2022) The Wall Heat Flux Partitioning during the Pool Boiling of Water on Thin Metallic Foils. *Applied Thermal Engineering*, **200**, Article ID: 117638. https://doi.org/10.1016/j.applthermaleng.2021.117638

[14] Jayaramu, P., Gedupudi, S. and Das, S.K. (2019) An Experimental Investigation on the Influence of Copper Ageing on Flow Boiling in a Copper Microchannel. *Heat Transfer Engineering*, **41**, 333-350. https://doi.org/10.1080/01457632.2018.1540459

[15] Jayaramu, P., Jain, S., Gedupudi, S. and Das, S.K. (2021) Experimental Investigation on the Change in Flow Boiling Characteristics Due to Boiling-Induced Copper Ageing. *Journal of Heat Transfer*, **143**, Article ID: 074502. https://doi.org/10.1115/1.4051124

[16] Sielaff, *et al*. (2022) The Multiscale Boiling Investigation On-Board the International Space Station: An Overview. *Applied Thermal Engineering*, **205**, Article ID: 117932. https://doi.org/10.1016/j.applthermaleng.2021.117932

[17] Janna, W.S. (2009) Engineering Heat Transfer. 3rd Edition, CRC Press, Boca Raton, Chapter 10.

[18] Adesope, O.O., Pour, N.B., Van Wie, B.J. and Thiessen, D.B. (2019) Work in Progress: Fostering Cognitive Engagement with Hands-On Learning Pedagogy. 2019 *ASEE Annual Conference & Exposition*, Tampa, Florida, June 15, 2019, Paper ID #27012

[19] Dahlke, K., Kaiphanliam, K., Van Wie, B.J., Thiessen, D.B., Dutta, P., Adesope, O. and Reynolds, O. (2020) A First Year Progress Report on "Collaborative Research: Using Low Cost Desktop Learning Modules to Educate Diverse Undergraduate Communities in Engineering". 2020 *ASEE Virtual Annual Conference Content Access*, 22-26 June 2020, Paper ID #31281.

[20] Pour, N.B., Van Wie, B.J., Kaiphanliam, K., Khan, A.I., Dutta, P., Reynolds, O., Dahlke, K., Adesope, O., Oje, O. and Gartner, J.B. (2020) Design Philosophy and System Integrity for Propagation of Hands-On Desktop Learning Modules for Fluid Mechanics and Heat Transfer. 2020 *ASEE Virtual Annual Conference Content Access*, 22-26 June 2020, Paper ID #30913.

[21] Toro, X., Compere, M., Van Wie, B. and Dikici, B. (2011) A Solar-Powered Direct Steam Generation Boiler for an Educational Desktop Rankine Cycle. *ASME* 2011 *International Mechanical Engineering Congress and Exposition*, Denver, 11-17 November 2011, 241-248. https://doi.org/10.1115/IMECE2011-63699

[22] Dikici, B. and Al-Sukaini, B.Q. (2016) Pool Boiling Heat Transfer Enhancement with Structured Surfaces. *Proceedings of ASME Power and Energy Conference and Exhibition*, Charlotte, 26-30 June 2016, V001T01A004. https://doi.org/10.1115/POWER2016-59364

[23] Cengel, Y. (2002) Heat Transfer: A Practical Approach. 2nd Edition, McGraw-Hill, New York.

[24] Thermal-Fluids Central, Pool Boiling Regimes. http://www.thermalfluidscentral.org/encyclopedia/index.php/Pool_Boiling_Regimes

[25] Kruse, C.M. anderson, T., Wilson, C., Zuhlke, C., Alexander, D., Gogos, G. and Ndao, S. (2018) Enhanced Pool-Boiling Heat Transfer and Critical Heat Flux on Femtosecond Laser Processed Stainless Steel Surfaces. *International Journal of Heat and Mass Transfer*, **82**, 109-116. https://doi.org/10.1016/j.ijheatmasstransfer.2014.11.023

[26] Ravikumar, S.V., Jha, J.M., Sarkar, I., Mohapatra, S.S. and Pal, S.K. (2013) Achievement of Ultrafast Cooling Rate in a Hot Steel Plate by Air-Atomized Spray with Different Surfactant Additives. *Experimental Thermal and Fluid Science*, **50**, 79-89. https://doi.org/10.1016/j.expthermflusci.2013.05.007

[27] Pioro, I.L. (1999) Experimental Evaluation of Constants for the Rohsenow Pool Boiling Correlation, *International Journal of Heat and Mass Transfer*, **42**, 2003-2013. https://doi.org/10.1016/S0017-9310(98)00294-4

[28] Das, A.K., Das, P.K. and Saha, P. (2007) Nucleate Boiling of Water from Plain and Structured Surfaces. *Experimental Thermal and Fluid Science*, **31**, 967-977. https://doi.org/10.1016/j.expthermflusci.2006.10.006

[29] Jabardo, J.M.Z., Silva, E.F.S., Ribatski, G. and Barros, S.F.B. (2004) Evaluation of the Rohsenow Correlation through Experimental Pool Boiling of Halocarbon Refrigerants on Cylindrical Surfaces. *Journal of the Brazilian Society of Mechanical Sciences and Engineering*, **26**, 218-230. https://doi.org/10.1590/S1678-58782004000200015

[30] Dhir, V.K. (1998) Boiling Heat Transfer. *Annual Review of Fluid Mechanics*, **30**, 365-401. https://doi.org/10.1146/annurev.fluid.30.1.365